An experimental study of rill erosion and morphology

Haiou Shen [a,b], Fenli Zheng [a,b,*], Leilei Wen [a,b], Jia Lu [b,c], Yiliang Jiang [b,c]

[a] College of Natural Resources and Environment, State Key Laboratory of Soil Erosion and Dryland Farming on the Loess Plateau, Northwest A & F University, Yangling, Shaanxi 712100, PR China
[b] Institute of Soil and Water Conservation, CAS & MWR, Yangling, Shaanxi 712100, PR China
[c] Institute of Soil and Water Conservation, Northwest A & F University, Yangling, Shaanxi 712100, PR China

ABSTRACT

Rill erosion is recognized as an important process of water erosion on agricultural land. The objectives of this study are to examine the effects of rainfall intensity on rill network development and to present some indicators for a quantitative description of rill morphology. A soil pan (10 m long, 3 m wide and 0.5 m deep and with an adjustable slope gradient from 0 to 30°) was subjected to three successive rains under rainfall intensities of 50 and 100 mm h^{-1}. The results showed that rainfall intensity significantly affected rill erosion, especially in the active period of rill network development. The magnitude of rill erosion was 28.5 and 33.1 kg m^{-2} and contributed 78.6% and 76.2% to the soil loss under rainfall intensities of 50 and 100 mm h^{-1}, respectively. The formation of rill network under the 50 mm h^{-1} intensity was more complex than that under the 100 mm h^{-1} intensity; for the latter rill networks developed fast and then varied slightly. The mean rill inclination angle (δ_{mean}), rill density (ρ), degree of rill dissection (μ) and mean rill tortuosity complexity (c_{mean}) increased with the increase of rains under the same rainfall intensity. The μ value was the optimal derivative morphological indicator to estimate rill erosion and morphology, which was followed in descending order by δ_{mean}, c_{mean} and ρ.

© 2015 Elsevier B.V. All rights reserved.

1. Introduction

Rill erosion is a major soil erosion process caused by water on sloping croplands and rangelands in many areas around the world and causes much soil loss (Cai et al., 2004; Kimaro et al., 2008). It is geomorphologically important because it produces erosion features and resultant rill transport materials supplied by interrill erosion (Bewket and Sterk, 2003). Many studies have focused on rill erosion processes (Bryan and Rockwell, 1998; Wirtz et al., 2012). However, there are some differences in results depending on specific experiments, soil types, rainfall conditions and spatial scales (Devente and Poesen, 2005; Govers et al., 2007). Therefore, rill erosion is still one of the current research hotspots.

Rill networks develop with varying complexity (Brunton and Bryan, 2000; Mancilla et al., 2005). Rill network development leads to an increase in runoff connectivity and concentration of water flow along the channeling network (Heras et al., 2011). Quantitative measurements of rills include those of rill width, depth, and the width-to-depth ratio, as well as space filling tendencies of the networks (Raff et al., 2004). A rill network tends to fill the drainage area more completely with time.

The existing results usually focus on main rills, which transport most surface runoff and sediment out of the plot and are usually larger than the rest of the finer channels. Most studies have generally ignored secondary rills, which are small channels that usually transport less surface runoff than main rills or dissipate before reaching the plot outlet (Mancilla et al., 2005). However, this exclusion of secondary rills neglects an important part of the rill network.

Rill morphology plays a significant role in determining surface runoff and soil loss from hillslopes (Govindaraju and Kavvas, 1994). Flows in rills have higher velocities and transport significantly more sediment downslope than overland flows (Gatto, 2000). Eroding rills evolve morphologically in time and space (Lei and Nearing, 1998), and it is necessary to consider temporal and spatial variations (Boardman, 2006). Microtopography caused by rill erosion is often complicated and irregular, and a rill-by-rill survey is difficult and especially impractical in the field. The stochastic method was adopted to characterize rill morphology at various cross-slope locations along a hillslope (Govindaraju and Kavvas, 1994). Experiments on rill morphology at the field scale are essentially limited to qualitative or semi-quantitative descriptions (Bewket and Sterk, 2003).

Rill length and cross-sections are employed as indicators of rill morphology, where rill length is usefully chosen to describe the rilling process (Bruno et al., 2008) and is also a major component of rill volume variability on a watershed scale (Ludwig et al., 1995). Rill width and

depth are measured and interpolated along the incision network for calculation of the erosion rate (Cerdan et al., 2002).

Researchers have attempted to use rill density to characterize the erosion process (Gilley et al., 1990). However, there is an opposing view that rill density is insufficient to describe rill structure (Govindaraju and Kavvas, 1994). Rill horizon density (Wu et al., 1997) represents rill erosion intensity and morphology. Bewket and Sterk (2003) defined the area of actual damage as the surface area covered by rills.

To promote process studies of rill erosion, quantitative descriptions of rill morphology are useful. Therefore, a laboratory study with detailed measurements was conducted under controlled experimental conditions. Rill density (ρ) was used to characterize rill erosion; in addition, degree of rill dissection (μ), rill inclination angle (δ) and rill tortuosity complexity (c) were chosen to investigate characteristics of rill morphology and to quantify the evolution of rill networks on the hillslope. The objectives of this study are to investigate the effects of rainfall intensity on rill erosion and morphology, to present temporal and spatial variations of rill networks by using morphological indicators, analyze correlations between rill erosion and morphological indicators and propose the optimal indicator.

2. Materials and methods

2.1. Experimental materials

The simulated rainfall experiments were completed in the rainfall simulation laboratory of the State Key Laboratory of Soil Erosion and Dryland Farming on the Loess Plateau, Yangling City, China. The experiments were conducted in a slope adjustable pan, which was 10 m long, 3 m wide, 0.5 m deep and with many holes (2 cm aperture) at the bottom to facilitate drainage. The slope gradient ranged from 0 to 30° with adjustment steps of 5°. In this study, the soil pan was set at a slope of 20°. A down sprinkler rainfall simulator system (Zheng and Zhao, 2004) was used to apply rainfall. The rainfall simulator, which includes three nozzles, can be set to any selected rainfall intensity ranging from 30 to 350 mm h^{-1} by adjusting the nozzle size and water pressure. The fall height of the raindrops is 18 m above the ground, which allows all raindrops to reach the terminal velocity prior to impact. The simulated raindrop diameter distribution was 0.2–3.1 mm, and >85% of raindrop diameters were <1.0 mm. According to Chen and Wang (1991), most raindrop diameters from natural rain were also <1.0 mm. Thus, the simulated raindrop size could successfully replicate the natural raindrop size.

The soil used in this study was the loessial soil with 28.3% sand (>50 μm), 58.1% silt (50–2 μm), 13.6% clay (<2 μm) and 5.9 g kg^{-1} soil organic matter. The methods used to analyze soil texture and soil organic matter were the pipette method and the potassium dichromate oxidation-external heating method, respectively (Liu, 1996). The tested soil was collected from 0 to 20 cm in the Ap horizon of a well-drained site in Ansai, Shaanxi Province, China. Impurities, such as organic matters and gravels, were removed from all the soil, but the soil was not passed through any sieve to keep the natural state of the soil.

2.2. Preparation of the soil pan

Before packing the soil pan, the soil water content of the tested soil was determined, which was used to calculate how much soil was needed for packing the soil pan to obtain target soil bulk densities for different layers. First, a 5-cm-thick layer of sand was packed at the bottom of the soil pan that allowed free drainage of excess water. Then, the layers over the sand layer were divided into the plow pan with a depth of 15 cm and the tilth layer with a depth of 20 cm to simulate local sloping croplands; the bulk densities for the plow pan and the tilth layer were 1.35 and 1.10 g cm^{-3}, respectively. During the packing process, both the plow pan and the tilth layer were packed in 5-cm increments, and

each packed soil layer was raked lightly before the next layer was packed to ensure uniformity and continuity in the soil structure. The soil amount of each layer was kept as constant as possible to maintain similar bulk density and uniform spatial distribution of soil particles. After completion of packing the soil pan, a manual tillage on the soil pan was performed at an approximately 20 cm depth along the contour line, which is similar to the plowing depth of croplands. After plowing, the soil pan was allowed to settle for 48 h.

2.3. Experimental procedures

Before runs, the experimental soil pan was subjected to a pre-rain with the 30 mm h^{-1} rainfall intensity until surface flow occurred; the duration of this pre-rain was approximately 25 min. The purposes of the pre-rain were to maintain consistent soil moisture, consolidate loose soil particles by rainfall wetting, and reduce the spatial variability of surface conditions. The soil surface was covered with a plastic sheet after the pre-rain to prevent soil moisture evaporation and surface sealing, and allowed to stand for 24 h.

Prior to the experiment, rainfall intensity was calibrated to confirm the run-rainfall intensity reaching the target rainfall intensity and meeting experimental requirements; uniformity was >90%. The designed two rainfall intensities of 50 and 100 mm h^{-1} were used in this study, while a total rainfall of 50 mm was maintained during each treatment of both rainfall intensities; thus, rainfall durations were 60 min for 50 mm h^{-1} and 30 min for 100 mm h^{-1}. For better development of rill networks, each rainfall intensity experiment contained three successive rains (i.e., 1st to 3rd rains) with an interval of 24 h, respectively.

2.4. Experimental measurements

2.4.1. Runoff and soil loss

One day after the pre-rain, the designed rainfall intensity (50 or 100 mm h^{-1}) was applied to the soil pan. For each treatment, after runoff occurred, runoff samples were collected in 15-liter buckets, and the samples were measured in 1 or 2 min intervals for the whole rainfall durations, with 30 min for 100 mm h^{-1} and 60 min for 50 mm h^{-1}, respectively. These samples were weighed and then oven-dried at 105 °C to calculate sediment yield.

2.4.2. Rill development

Manual measurements of each rill's length, width, depth and locations (x, y) along with rainfall duration, were performed when rills were generated. To aid in recognizing these rills, photographs were taken of the soil pan surface at different times throughout each rain. After the completion of each rain, the rill network was mapped in detail. Rill width and depth measurements were conducted along each rill channel at intervals of 5 or 10 cm. Furthermore, these measurements were also performed once sudden changes in the rill pattern occurred (Øygarden, 2003).

2.5. Defining derivative morphological indicators

Rill length, width and depth are the basic morphological indicators, which are directly measured and used to calculate other derivative morphological indicators. In this study, four derivative morphological indicators were chosen and defined to describe rill morphology.

2.5.1. Rill inclination angle

The rill inclination angle along the hillslope (δ, in degrees) is an average angle between directions of a rill at measurement points and the vertical direction of the rill. It reflects the ductility of a rill in the horizontal and vertical directions. In general, if δ is larger, runoff and sediment have a stronger conductivity in the horizon direction. On the contrary, if δ is smaller, a greater degree of vertical extension of a rill

occurs, where runoff and sediment transport occur more smoothly and with a higher connectivity. The specific formula is:

$$\delta = \sum_{i=1}^{m} \theta_i \Big/ m \tag{1}$$

where θ_i is the angle between the direction of a rill at each turn and the vertical direction of the rill (in degrees); and $i = 1, \ldots, m$ represents the number of measurement points, as shown in Fig. 1.

2.5.2. Rill density

Rill density (ρ) is the total rill length divided by the total catchment area (m m^{-2}) (Bewket and Sterk, 2003). It is a measure of how well or poorly a catchment is drained by rill channels. The ρ value depends on slope gradient, slope length, rainfall intensity, soil permeability and other catchment characteristics. It reflects the degree of fragmentation. Higher ρ indicates a greater soil erosion rate and a high bifurcation ratio. The ρ value is suitable for roughly describing rill morphology. The formula is:

$$\rho = \sum_{j=1}^{n} L_{tj} \Big/ A_0 \tag{2}$$

where A_0 is the plane area of the total studied catchment (m^2); L_{tj} is the total length of a rill and its bifurcations (m); and $j = 1, \ldots, n$ represents the number of rills in the studied area.

2.5.3. Degree of rill dissection

The degree of rill dissection (μ) is rill coverage area per unit drainage area. It is a dimensionless factor with similarities to and differences from ρ. The μ value considers both rill length and width, and more directly reflects the distribution of rills on the hillslope than ρ, which only considers length. A higher μ value represents more fragmented rills and greater rill erosion intensity in the drainage area. The specific formula is:

$$\mu = \sum_{j=1}^{n} A_j \Big/ A_0 \tag{3}$$

where A_j is the plane area of the j-th rill (m^2).

2.5.4. Rill tortuosity complexity

The rill tortuosity complexity (c) is the ratio of the total length of a rill and its bifurcations to the vertical effective length of the rill. The c value indicates areas affected by the rill in the catchment. It is a dimensionless factor larger than the unity. There is a certain relationship between c and its vertical effective length; in concept, they are inversely proportional. However, a shorter rill tends to have fewer bifurcations, its expansive range in the catchment is smaller, and c is therefore smaller. The longer the vertical effective length, the more complex the actual path of the rill, which may have a broad extension in the drainage area, resulting in a larger c value. The formula is:

$$c = L_{tj}/L_j \tag{4}$$

where L_j is the vertical effective length of the j-th rill (m).

3. Results and discussion

3.1. Runoff and soil loss

Table 1 shows runoff, soil loss and rill erosion for three successive rains with rainfall intensities of 50 and 100 mm h^{-1}, respectively. Runoff at the 1st rain was lower compared with the 2nd and 3rd rains under the two rainfall intensities. Although the pre-rain was conducted before the 1st rain for all experimental treatments, the soil profile in the soil pan remained unsaturated. Thus, a portion of the rainfall infiltrated at the earlier stage of the 1st rain under the two rainfall intensities; then the soil infiltration reached to the stable infiltration rate in the later stage of the 1st rain, which caused runoff rate in the 2nd and 3rd rains of both rainfall intensities to be larger. Although the development of rill networks was different in the 2nd and 3rd rains of the two rainfall intensities, there was no significant difference in runoff rate between the two rains.

Soil loss increased with the increase of rains at the 50 mm h^{-1} intensity (Table 1). Compared with the 1st rain, soil loss for the 2nd rain sharply rose by 59.3%, and there was no significant difference between the later two rains. Soil loss at the 100 mm h^{-1} rainfall intensity decreased in the order of 2nd > 3rd > 1st, where the 2nd rain produced the highest soil loss and had a significant difference compared with the other two rains. The 1st rains of both rainfall intensities produced the lower soil loss. The reason was that splash erosion played a major role on the hillslope at the beginning of the 1st rain; once surface flow occurred with the rainfall process, sheet erosion immediately appeared. Compared with rill erosion, splash erosion and sheet erosion produced relatively lower soil loss. Once rill erosion occurred and became the dominant erosion pattern, soil loss rapidly increased. Field surveys and experimental results also showed that the occurrence of rill erosion increased soil loss several times or more (Govers and Poesen, 1988; Kimaro et al., 2008). Regarding the 2nd and 3rd rains of both rainfall intensities, rill erosion was dominant on the hillslope. These results showed that an increase in runoff does not always coincide with an increase in soil loss and vice versa (Nord and Esteves, 2010).

Table 1 shows that soil loss at 100 mm h^{-1} was 1.56 times higher than that at 50 mm h^{-1} in the 1st rain; this decreased to 1.18 times in the 2nd rain; while in the 3rd rain, soil loss caused by 50 and
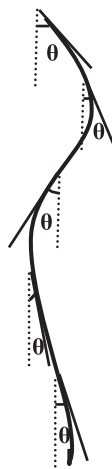
—— The direction at each turn

········· The vertical direction along the hillslope

Fig. 1. Schematic diagram of rill inclination angle.

Table 1
Runoff, soil loss and rill erosion for the three successive rains at rainfall intensities of 50 and 100 mm h^{-1}.

Rainfall intensity (mm h^{-1})	Successive rains	Rainfall duration (min)	Runoff (mm)	Soil loss (kg m^{-2})	Rill erosion (kg h^{-2})	Occupying percent of rill erosion (%)
50	1st	60	33.9 a	8.6 a	5.3 a	61.8
	2nd	60	47.5 b	13.7 b	11.1 b	80.9
	3rd	60	48.8 b	14.0 b	12.1 b	86.7
100	1st	30	36.3 a	13.4 a	10.2 a	75.9
	2nd	30	46.9 b	16.2 b	12.0 a	73.9
	3rd	30	47.4 b	13.8 a	10.9 a	79.0

Means values for a treatment followed by an identical letter (a or b) are not significantly different at $P < 0.05$ according to the LSD test.

Fig. 2. Initial surface and rill networks after each rain at the 50 mm h^{-1} rainfall intensity.

Fig. 3. Initial surface and rill networks after each rain at the 100 mm h^{-1} rainfall intensity.

Table 2
Rill length, mean rill width and depth for the three successive rains at rainfall intensities of 50 and 100 mm h^{-1}.

Simulated rainfall	50 mm h^{-1}			100 mm h^{-1}		
	1st rain	2nd rain	3rd rain	1st rain	2nd rain	3rd rain
Rill length (m)	41.4	63.2	67.4	56.4	74.1	77.4
Mean rill width (cm)	7.2	10.1	12.9	9.0	10.7	12.9
Mean rill depth (cm)	5.0	7.4	9.3	6.1	8.0	9.7

100 mm h^{-1} rainfall intensities was similar. This result indicates that rainfall intensity played a major role in soil erosion. Generally, the larger rainfall intensity would result in greater soil loss in the case of the same rainfall, especially in the early stage of soil erosion. Rainfall intensity affected soil erosion by infiltration and runoff (Wang et al., 1995). There were certain amounts of infiltration in the 1st rain under the two rainfall intensities, but runoff erosivity at the 100 mm h^{-1} intensity, which caused much more soil loss, was apparently higher than that at the 50 mm h^{-1} intensity once rill erosion occurred. Along with the increase of rains under the same rainfall intensity, rill network development tended to reach maturity, and the remaining erodible soils decreased. Thus, the increment of soil loss from the 2nd rain at the 100 mm h^{-1} intensity was lower than that at the 50 mm h^{-1} intensity.

The changing trend of rill erosion was similar to that of soil loss at the 50 mm h^{-1} rainfall intensity (Table 1). However, there were no significant differences in rill erosion between the three successive rains at the 100 mm h^{-1} intensity. By combining the three successive rains, the magnitude of rill erosion was 28.5 and 33.1 kg m^{-2} under rainfall intensities of 50 and 100 mm h^{-1}, respectively. Contributions of rill erosion to soil loss increased from 61.8% to 80.9%, and then 86.7% with increasing successive rains at the 50 mm h^{-1} intensity. Rill erosion at the 100 mm h^{-1} intensity accounted for 75.9% of soil loss for the 1st rain, but it slowly decreased to 73.9% for the 2nd rain and then rose to 79.0% for the 3rd rain. Rill erosion contributed 78.6% to soil loss at the 50 mm h^{-1} intensity and 76.2% at the 100 mm h^{-1} intensity as a whole. This result was similar to that obtained by Zheng et al. (1987), who noted that rill erosion accounted for 74.2% of hillslope soil loss. The results of this study showed that contributions of rill erosion to soil loss were quite high, especially in the later two rains at the rainfall intensity of 50 mm h^{-1}, which were even higher than those at the intensity of 100 mm h^{-1}. The reason was that the 100 mm h^{-1} intensity produced much more rainfall erosivity and runoff erosivity, which would increase the proportion of interrill erosion compared with the 50 mm h^{-1} intensity, even though the 100 mm h^{-1} intensity produced much more rill erosion due to larger runoff erosivity.

Although the same rainfall intensity was designed for the three successive rains, runoff, soil loss and rill erosion changed not only for impacts of infiltration and erosion patterns, but also for different initial surface erosion morphology. The 1st rain was conducted on a hillslope with a plane surface, the 2nd rain was on the basis of the rill morphology formed by the 1st rain, and the 3rd rain was on the basis of the rill morphology formed by the first two rains. Therefore, soil resistance changed, runoff resistance decreased, concentrated flow increased and erosivity increased in the later rains. As a result, rills were lengthening,

widening, deepening and rapidly developing. The surface erosion morphology led to flow convergence and divergence, resulting in a non-uniform distribution of rill spacing and efficiency (Rieke-Zapp and Nearing, 2005).

3.2. Rill morphology

3.2.1. Rill network formation

At the earlier stage of the 1st rain and before runoff occurred, splash erosion played a major role on the hillslope. With the rainfall process, surface flow formed and sheet erosion occurred. Then, surface flow gradually converted into concentrated flow, which was the main cause of rill erosion (Owoputi and Stolte, 1995). In the concentrated flow path, runoff erosivity increased enough to scour soil clods, which resulted in small waterfalls. Then, once small waterfalls evolved into rill headcuts, rill erosion correspondingly occurred. Undercut erosion of headcuts, headward erosion of rill head and side-wall collapse erosion conduced discontinuous rills. After that, the connection of multiple discontinuous rills on the same concentrated flow path formed a continuous rill by headward erosion (Zheng et al., 1987). During this process, differences in the erosivity of rainfall and runoff and soil resistance in space and time resulted in the phenomena of bifurcation, combination and connectivity. All of these processes both promoted rill network development and intensified rill erosion.

After the 1st rain, there were small rills and waterfalls along the hillslope, and the initial rill network had been formed (Figs. 2 and 3). Then, after the 2nd rain, the rill network further developed. After the 3rd rain, there were certain changes in rill width and depth. Although morphological changes were similar for the two rainfall intensities, there were some differences specific to rill length, width, depth and other quantitative indicators as discussed below.

3.2.2. Rill length, width and depth statistics

Rill length for the three successive rains of both rainfall intensities is presented in Table 2. Rill length increased with the increase of rains, but the increment gradually decreased. Additionally, rill length at the 100 mm h^{-1} rainfall intensity was longer than that at the 50 mm h^{-1} intensity for each rain. After the 1st rain, rill length at 100 mm h^{-1} was 1.36 times longer than that at 50 mm h^{-1}. However, for the later two rains, the increased rill lengths at 100 mm h^{-1} were both shorter than those at 50 mm h^{-1}. This result indicates that the effects of rainfall intensity on rill length were mainly reflected in the early stage of soil erosion, when development of the rill network was active and headward erosion played a dominant role; which resulted in the rapid increase in the total length of all rills. Compared with the 50 mm h^{-1} rainfall intensity, there was a shorter active period of rill network development at the 100 mm h^{-1} intensity, but rill length increased faster. Then, rill erosion gradually reached a relatively stable stage; headward erosion became weak and the increment of rill lengths slowed down. The main processes of rill lengthening were headward erosion and connections of a few rills on the same concentrated flow path.

The mean rill width and depth increased with the increase of rains under the same rainfall intensity (Table 2), but were different between the two rainfall intensities. Generally, the mean rill width and depth at

Table 3
Frequency statistics of rill width for the three successive rains at rainfall intensities of 50 and 100 mm h^{-1}.

Rainfall intensity (mm h^{-1})	Successive rains	Sample numbers[a]	Frequency statistics of rill width (%)						
			≤5 cm	5–10 cm	10–15 cm	15–20 cm	20–25 cm	25–30 cm	>30 cm
50	1st	458	45.6	37.3	10.0	5.2	1.1	0.7	0
	2nd	614	32.4	32.1	15.3	10.9	5.5	2.8	1.0
	3rd	640	22.0	25.0	19.2	16.3	8.1	6.1	3.3
100	1st	576	28.8	38.7	21.2	8.9	1.6	0.7	0.2
	2nd	733	25.5	31.5	21.3	12.7	6.0	2.3	0.7
	3rd	748	17.5	25.9	24.5	16.4	9.0	5.5	1.2

[a] Number of measurement points.

the 100 mm h^{-1} rainfall intensity were larger than at the 50 mm h^{-1} intensity for each corresponding rain, and differences in mean rill width or depth for the two rainfall intensities became smaller with the increase of rains. Taking mean rill width as the example, the mean rill width at 100 mm h^{-1} were 1.25 and 1.06 times wider than those at 50 mm h^{-1} for the 1st and 2nd rains, respectively. The changing trend of mean rill depth was similar to the mean rill width. The above results indicate that there were important effects of rainfall intensity on rill width and depth, but they decreased with the increase of rains because rill network development gradually tended to reach maturity.

Frequency statistics of rill widths showed that the proportions of rill widths <5 cm and 5–10 cm decreased, and the other sections gradually increased with the increase of rains at the same rainfall intensity (Table 3). Regarding the 50 mm h^{-1} rainfall intensity, most rill widths after the 1st rain were <15 cm, which occupied 93.0% of the total and the distribution in the range <10 cm was 83.0%. There was no rill width >30 cm. Rill widths became larger after the 2nd and 3rd rains. After the 2nd rain, nearly 90.7% of rill widths were <20 cm and 8.3% were 20–30 cm. Only a few rill widths were ≥30 cm. After the 3rd rain, the proportion of rill widths <20 cm decreased by 9.1%, and larger rill widths increased. The frequency of rill widths at 100 mm h^{-1} rainfall intensity had a similar distribution pattern. However, rill widths at 100 mm h^{-1} were generally larger than those at 50 mm h^{-1}. Zheng et al. (1987) noted that rill widths could reach 50 cm but mostly <30 cm. In this study, most rill widths were <20 cm for the two rainfall intensities; only a few rill widths exceeded 30 cm, which were located at specific sections where side-walls collapsed. The main processes of rill widening were the collapse of side-wall small clods and the combination of neighboring rills.

Table 4 shows the results of the frequency statistics of rill depth for the three successive rains of both rainfall intensities. Rill depth became larger with the increase of rains and rainfall intensities. Most rill depths were <20 cm, which was similar to the results of Zheng et al. (1987), according to field investigations and rainfall simulations. However, there were some differences in rill depths specific to each rain. Rill depths <10 cm were dominant after the 1st rain and occupied 93.9% and 92.5% of all rill depths at the 50 and 100 mm h^{-1} rainfall intensity, respectively. Moreover, most rill depths were <15 cm even after the 2nd and 3rd rains of both rainfall intensities. There was only a small portion of rill depths >20 cm for all rains. When the rill cut down to the plow pan, the cut-down rate of the rill depth became slow. The shoulder would develop in rills, which was represented on the top of the plow pan. This was similar to the field observations by Fullen (1985). The main process of rill deepening was the undercut erosion, especially for the undercut erosion of additional headcuts in the rill.

3.3. Quantitative description of rill morphology

3.3.1. Rill inclination angle

The mean rill inclination angle (δ_{mean}) increased with the increase of rains, but it was greater at the 50 mm h^{-1} rainfall intensity than that at the 100 mm h^{-1} intensity (Table 5). After the 1st rain, the rill network at 100 mm h^{-1} was slightly more complex than that at 50 mm h^{-1}. However, as mentioned earlier, there were much more serious side-

Table 5
Derivative morphological indicators for the three successive rains at rainfall intensities of 50 and 100 mm h^{-1}. δ_{mean}: mean rill inclination angle; ρ: rill density; μ: degree of rill dissection; c_{mean}: mean rill tortuosity complexity.

Rainfall intensity (mm h^{-1})	Successive rains	δ_{mean} (°)	ρ (m m^{-2})	μ	c_{mean}
50	1st	18.1	1.38	0.10	1.10
	2nd	20.2	2.11	0.20	1.23
	3rd	22.1	2.25	0.28	1.35
100	1st	19.5	1.88	0.16	1.24
	2nd	19.9	2.47	0.25	1.27
	3rd	20.8	2.58	0.31	1.30

wall collapses at the 100 mm h^{-1} rainfall intensity than those at the 50 mm h^{-1} intensity. Side-wall collapses tended to make rills relatively straighter. Thus, δ_{mean} after the 2nd or 3rd rains at the 100 mm h^{-1} intensity were smaller than that at the 50 mm h^{-1} intensity.

The change of δ_{mean} for the three successive rains of the same rainfall intensity illustrates that rill development tended to form the complex network, rather than to parallel. Runoff preferred the path with less resistance, and flowed out according to the most favorable direction corresponding to the theory of minimum energy dissipation. Therefore, some small rills had greater plasticity and would move close to the neighboring main rills, and then, δ_{mean} became larger with increasing rainfall duration until the rill network fully developed.

The mean reflects the overall level of δ. Nevertheless, the specific distribution of δ is necessary. Hence, the ranges of δ versus rains are plotted in Fig. 4. All three successive rains under both rainfall intensities of 50 and 100 mm h^{-1} were taken into account. Concerning the 50 mm h^{-1} intensity, the highest range between the maximum and minimum values belonged to the 2nd rain. The inter-quartile (the range between the 75% and 25% quartiles) increased with the increase of rains. Seventy-five percent of the values of δ were <25° for the 1st and 2nd rains and <27° for the 3rd rain. The medians of δ also increased with the increase of rains and varied between 15 and 20°. For the 100 mm h^{-1} intensity, the ranges between maximum and minimum values slightly ascended for the three successive rains. For the 1st rain, the range between maximum and minimum values at the 100 mm h^{-1} intensity was greater than that at 50 mm h^{-1}. But for the 2nd and 3rd rains, the range at 100 mm h^{-1} was lower than that at 50 mm h^{-1}. The inter-quartile did not present regularity at the 100 mm h^{-1} rainfall intensity, whereas it was higher than that at the 50 mm h^{-1} intensity for each rain. Additionally, the medians of δ also varied between 15 and 20°. In summary, most δ values concentrated between 15 and 25° for the three successive rains under the both rainfall intensities. The above results illustrates that the 50 mm h^{-1} rainfall intensity was conducive to the development of rill inclination, and sometimes extreme values of δ would appear. The rill network formed quickly under the 100 mm h^{-1} intensity, but the probability of exhibiting extreme values of δ was smaller.

3.3.2. Rill density

The ρ values for six rill networks are listed in Table 5 and they increased with the increase of rains and rainfall intensities. The greater

Table 4
Frequency statistics of rill depth for the three successive rains at rainfall intensities of 50 and 100 mm h^{-1}.

Rainfall intensity (mm h^{-1})	Successive rains	Sample numbers[a]	Frequency statistics of rill depth (%)				
			≤5 cm	5–10 cm	10–15 cm	15–20 cm	>20 cm
50	1st	458	60.9	33.0	5.5	0.4	0.2
	2nd	614	36.2	37.8	23.8	2.3	0
	3rd	640	26.1	34.2	24.1	14.4	1.3
100	1st	576	44.6	47.9	7.5	0	0
	2nd	733	37.1	30.7	25.0	7.2	0
	3rd	748	30.3	26.9	23.0	18.0	1.7

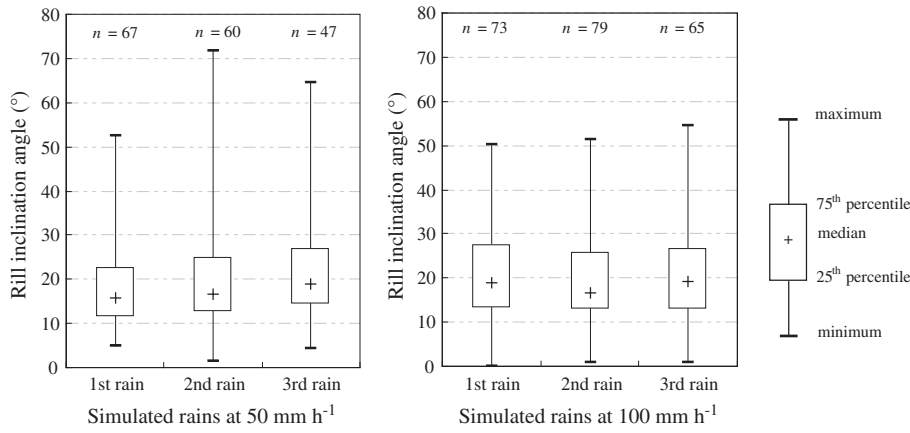[a] Number of measurement points.

Fig. 4. Ranges of the rill inclination angle for the three successive rains at rainfall intensities of 50 and 100 mm h^{-1}. n = the number of all rills on the hillslope.

ρ, the better drained the experimental soil pan. For the 50 mm h^{-1} rainfall intensity, ρ after the 2nd rain was 1.53 times greater than that after the 1st rain, and there was a smaller increment of ρ after the 3rd rain. For the 100 mm h^{-1} rainfall intensity, ρ increased by 36.2% after the 1st rain compared with that of the 50 mm h^{-1} intensity, and ρ after the 2nd rain was 1.31 times greater than that after the 1st rain. Likewise, there was a smaller difference in ρ between the 2nd and 3rd rains. The reason for these results was the same as the cause of changes in the total rill length mentioned above.

3.3.3. Degree of rill dissection

There were differences between μ and ρ. Although μ also increased with the increase of rains and rainfall intensities, the increment of μ was significantly higher than that of ρ (Table 5). The μ value of the latter rain was always higher than the former rain, with magnitudes 2.00 and 1.40 times larger at the 50 mm h^{-1} rainfall intensity and 1.56 and 1.24 times larger at the 100 mm h^{-1} intensity, respectively.

The μ value directly reflected the distribution of rills on the hillslope and illustrated how seriously the hillslope was fragmented by rill network development. It included both the effects of headward erosion and side-wall collapse. However, ρ just reflected the level of headward erosion. Therefore, μ is a better rill morphological indicator compared with ρ.

3.3.4. Rill tortuosity complexity

Table 5 shows that c_{mean} increased with the increase of rains at the same rainfall intensity. It was relatively smaller after the 1st rain for

the 50 mm h^{-1} rainfall intensity, and then gradually increased to 1.23 after the 2nd rain and 1.35 after the 3rd rain, with increases of 11.8% and 9.8%, respectively. The c_{mean} value after the 1st rain at the 100 mm h^{-1} rainfall intensity quickly reached 1.24, which was similar or even greater than that after the 2nd rain at the 50 mm h^{-1} intensity; whereas, c_{mean} increased slightly, and the value after the 3rd rain was even smaller than that at the 50 mm h^{-1} intensity. The above results indicate that the formation of rill networks at the 50 mm h^{-1} rainfall intensity was more complex than that at the 100 mm h^{-1} intensity; for the latter rill network developed fast and then varied slightly. The c value could measure how broad the extension was, and it was a better derivative morphological indicator for estimating the degree of rill development.

The value of c changed significantly or subtly according to the characteristics of the hillslope's microtopography, rainfall, slope gradient, and slope length. Table 5 only gives changes of the mean value of c. However, showing the specific values of c for all main rills for each rain, Fig. 5 makes the changes more intuitive. Concerning the 50 mm h^{-1} rainfall intensity, the ranges between maximum and minimum values, as well as the inter-quartile, increased progressively with the increase of rains. The 75 percentile of c was 1.14 after the 1st rain and then rose by 17.8% for the 2nd rain and then by 9.5% for the 3rd rain. The medians of c for the three successive rains were all <1.1. Regarding the 100 mm h^{-1} rainfall intensity, the ranges between maximum and minimum values also slightly ascended for the three successive rains. The ranges between maximum and minimum values were slightly greater than those at 50 mm h^{-1} for the 1st and 2nd rains and
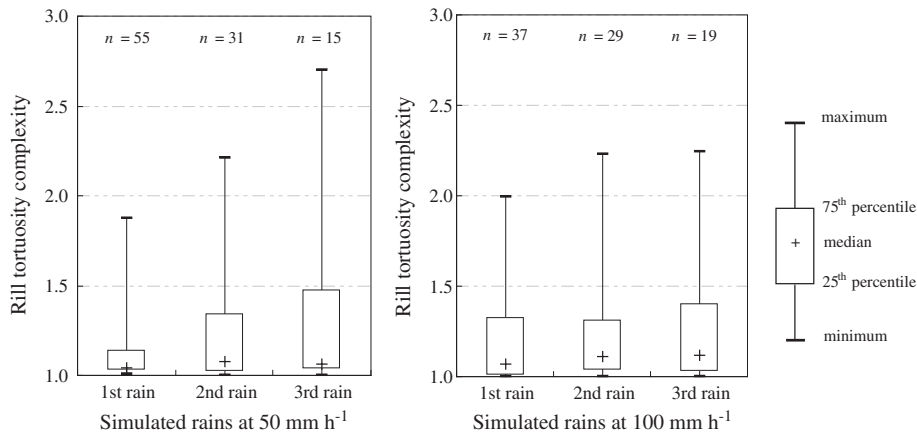

Fig. 5. Ranges of the rill tortuosity complexity for the three successive rains at rainfall intensities of 50 and 100 mm h^{-1}. n = the number of main rills, except their bifurcations, on the hillslope.

Table 6
Correlation matrix for rill erosion and each morphological indicator. SL: soil loss; RE: rill erosion rate; W_{mean}: mean rill width; D_{mean}: mean rill depth; δ_{mean}: mean rill inclination angle; ρ: rill density; μ: degree of rill dissection; c_{mean}: mean rill tortuosity complexity.

	SL	RE	W_{mean}	D_{mean}	δ_{mean}	ρ	μ	c_{mean}
SL	1	0.941**	0.755**	0.718*	0.519	0.502	0.667*	0.423
RE	0.941**	1	0.859**	0.773**	0.523	0.364	0.649*	0.352
W_{mean}	0.755**	0.859**	1	0.956**	0.696*	0.461	0.843**	0.511
D_{mean}	0.718*	0.773**	0.956**	1	0.797**	0.683*	0.955**	0.695*
δ_{mean}	0.519	0.523	0.696*	0.797**	1	0.757**	0.876**	0.851**
ρ	0.502	0.364	0.461	0.683*	0.757**	1	0.849**	0.912**
μ	0.667*	0.649*	0.843**	0.955**	0.876**	0.849**	1	0.836**
c_{mean}	0.423	0.352	0.511	0.695*	0.851**	0.912**	0.836**	1

$n = 12$.
* $P < 0.05$.
** $P < 0.01$.

significantly lower for the 3rd rain. The inter-quartile did not present any regularity at the 100 mm h^{-1} intensity, and it decreased in the order of 3rd > 1st > 2nd. The medians of c also increased with the increase of rains and were close to 1.1. In summary, most c values were <1.5 for all rains of both rainfall intensities. The degree of variation in c at the 50 mm h^{-1} rainfall intensity increased progressively and even exceeded that for the 100 mm h^{-1} intensity for later rains. The above results also illustrated that the 50 mm h^{-1} rainfall intensity was conducive to rill network development.

3.4. Correlations between rill erosion and morphological indicators

Above four derivative morphological indicators characterized rill erosion and morphology from different aspects. A correlation matrix of the Pearson correlation coefficient was used to analyze the correlations between soil loss, rill erosion rate and each morphological indicator (Table 6). Mean rill width (W_{mean}) and depth (D_{mean}), as the basic morphological indicators together with the above four derivative morphological indicators, were taken into account. There was a highly significant correlation between the rill erosion rate (RE) and soil loss (SL), whose correlation coefficient reached 0.941. This indicates that rill erosion intensity could reflect soil erosion intensity on the hillslope. Thus, rill erosion rate could substitute for soil loss for analyzing correlations with other indicators.

The strongest correlations were RE with W_{mean}, D_{mean} and μ (Table 6). The matrix illustrates that rill width was the best basic morphological indicator and degree of rill dissection was the best derivative morphological indicator to estimate the magnitude of soil loss and rill erosion. For the four derivative morphological indicators, the strongest correlations were also μ with the other indicators, thus, μ was the optimal indicator among four derivative morphological indicators to estimate rill morphology, which was followed in descending order by δ_{mean}, c_{mean} and ρ. Stronger correlations clearly reflect the availability of these selected derivative morphological indicators.

4. Conclusions

In this study, successive rainfall experiments focusing on rilling under rainfall intensities of 50 and 100 mm h^{-1} were conducted to investigate rill network development and a quantitative description of rill morphology. The results showed that rainfall intensity played a major role in rill erosion, especially in the active period of rill network development. By combining the three successive rains, the magnitude of rill erosion was 28.5 and 33.1 kg m^{-2} and contributed 78.6% and 76.2% to the soil loss under rainfall intensities of 50 and 100 mm h^{-1}, respectively. Most rill widths were <20 cm, and most rill depths were <15 cm. The values of δ_{mean}, ρ, μ and c_{mean} increased, along with the increase of rains under the same rainfall intensity. Most δ values concentrated from 15 to 25°, and most c values were <1.5. The formation of rill network at the 50 mm h^{-1} rainfall intensity was more complex than that at the 100 mm h^{-1} intensity; for the latter rill network developed

fast and then varied slightly. Furthermore, rill width was the best basic morphological indicator, and μ was the best derivative morphological indicator to evaluate rill erosion and morphology, which was followed in descending order by δ_{mean}, c_{mean} and ρ.

References

Bewket, W., Sterk, G., 2003. Assessment of soil erosion in cultivated fields using a survey methodology for rills in the Chemoga watershed, Ethiopia. Agric. Ecosyst. Environ. 97, 81–93.

Boardman, J., 2006. Soil erosion science: reflections on the limitations of current approaches. Catena 68, 73–86.

Bruno, C., Di Stefano, C., Ferro, V., 2008. Field investigation on rilling in the experimental Sparacia area, South Italy. Earth Surf. Process. Landf. 33, 263–279.

Brunton, D.A., Bryan, R.B., 2000. Rill network development and sediment budgets. Earth Surf. Process. Landf. 25, 783–800.

Bryan, R.B., Rockwell, D.L., 1998. Water table control on rill initiation and implications for erosional response. Geomorphology 23, 151–169.

Cai, Q.G., Zhu, Y.D., Wang, S.Y., 2004. Research on processes and factors of rill erosion. Adv. Water Sci. 15 (1), 12–18 (in Chinese, with English Abstract).

Cerdan, O., Le Bissonnais, Y., Couturier, A., Bourennane, H., Souchère, V., 2002. Rill erosion on cultivated hillslopes during two extreme rainfall events in Normandy, France. Soil Tillage Res. 67, 99–108.

Chen, W.L., Wang, Z.L., 1991. An experimental study of rainfall simulation characteristics. Bull. Soil Water Conserv. 11 (2), 55–62 (in Chinese, with English Abstract).

Devente, J., Poesen, J., 2005. Predicting soil erosion and sediment yield at the basin scale: scale issues and semi-quantitative models. Earth Sci. Rev. 71, 95–125.

Fullen, M.A., 1985. Compaction, hydrological processes and soil erosion on loamy sands in east Shropshire, England. Soil Tillage Res. 6, 17–29.

Gatto, L.W., 2000. Soil freeze–thaw-induced changes to a simulated rill: potential impacts on soil erosion. Geomorphology 32, 147–160.

Gilley, J.E., Kottwitz, E.R., Simanton, J.R., 1990. Hydraulic characteristics of rills. Trans. ASAE 33, 1900–1906.

Govers, G., Giménez, R., Van Oost, K., 2007. Rill erosion: exploring the relationship between experiments, modelling and field observations. Earth Sci. Rev. 84, 87–102.

Govers, G., Poesen, J., 1988. Assessment of the interrill and rill contributions to total soil loss from an upland field plot. Geomorphology 1, 343–354.

Govindaraju, R.S., Kavvas, M.L., 1994. A spectral approach for analyzing the rill structure over hillslopes. Part 1. Development of stochastic theory. J. Hydrol. 158, 333–347.

Heras, M.M.-d.l., Espigares, T., Merino-Martín, L., Nicolau, J.M., 2011. Water-related ecological impacts of rill erosion processes in Mediterranean-dry reclaimed slopes. Catena 84, 114–124.

Kimaro, D.N., Poesen, J., Msanya, B.M., Deckers, J.A., 2008. Magnitude of soil erosion on the northern slope of the Uluguru Mountains, Tanzania: interrill and rill erosion. Catena 75, 38–44.

Lei, T.W., Nearing, M.A., 1998. Rill erosion and morphological evolution: a simulation model. Water Resour. Res. 34, 3157–3168.

Liu, G.S., 1996. Soil Physical and Chemical Analysis and Description of Soil Profiles. Standards Press of China, Beijing, pp. 7–32 (in Chinese).

Ludwig, B., Boiffin, J., Chadoeuf, J., Auzet, A.-V., 1995. Hydrological structure and erosion damage caused by concentrated flow in cultivated catchments. Catena 25, 227–252.

Mancilla, G.A., Chen, S., McCool, D.K., 2005. Rill density prediction and flow velocity distributions on agricultural areas in the Pacific Northwest. Soil Tillage Res. 84, 54–66.

Nord, G., Esteves, M., 2010. The effect of soil type, meteorological forcing and slope gradient on the simulation of internal erosion processes at the local scale. Hydrol. Process. 24, 1766–1780.

Owoputi, L.O., Stolte, W.J., 1995. Soil detachment in the physically based soil erosion process: a review. Trans. ASAE 38, 1099–1110.

Øygarden, L., 2003. Rill and gully development during an extreme winter runoff event in Norway. Catena 50, 217–242.

Raff, D.A., Ramírez, J.A., Smith, J.L., 2004. Hillslope drainage development with time: a physical experiment. Geomorphology 62, 169–180.

Rieke-Zapp, D.H., Nearing, M.A., 2005. Slope shape effects on erosion: a laboratory study. Soil Sci. Soc. Am. J. 69, 1463–1471.

Wang, Z.G., Wei, Z.Y., Duan, X.M., Gao, C.Z., Wang, C.H., 1995. Study on sloping field erosion under simulated rainfall on Loess Broken Plateau—the comprehensive analysis of factors effected on rill erosion. J. Soil Water Conserv. 9 (2), 51–57 (in Chinese, with English Abstract).

Wirtz, S., Seeger, M., Ries, J.B., 2012. Field experiments for understanding and quantification of rill erosion processes. Catena 91, 21–34.

Wu, P.T., Zhou, P.H., Wu, C.L., Zheng, S.Q., Li, Y.Q., Ju, T.J., 1997. Research on the spatial distribution characteristics of slope rill erosion. Res. Soil Water Conserv. 4 (2), 47–56 (in Chinese, with English Abstract).

Zheng, F.L., Tang, K.L., Zhou, P.H., 1987. Approach to the genesis and development of rill erosion on slope land and the way to control. J. Soil Water Conserv. 1 (1), 36–48 (in Chinese, with English Abstract).

Zheng, F.L., Zhao, J., 2004. A brief introduction on the rainfall simulation laboratory and equipment. Res. Soil Water Conserv. 11 (4), 177–178 (in Chinese).